Single Molecular Spectroscopy: Identification of Individual Fullerene Molecules

Luiz H. G. Tizei, Zheng Liu, Masanori Koshino, Yoko Iizumi, Toshiya Okazaki, and Kazu Suenaga*
Nanotube Research Center, National Institute of Advanced Industrial Science and Technology (AIST), Tsukuba 305-8565, Japan
(Received 11 August 2014; published 29 October 2014)

We report the molecule-by-molecule spectroscopy of individual fullerenes by means of electron spectroscopy based on scanning transmission electron microscopy. Electron energy-loss fine structure analysis of carbon 1*s* absorption spectra is used to discriminate carbon allotropes with known symmetries. C_{60} and C_{70} molecules randomly stored inside carbon nanotubes are successfully identified at a single-molecular basis. We show that a single molecule impurity is detectable, allowing the recognition of an unexpected contaminant molecule with a different symmetry. Molecules inside carbon nanotubes thus preserve their intact molecular symmetry. In contrast, molecules anchored at or sandwiched between atomic BN layers show spectral modifications possibly due to a largely degraded structural symmetry. Moreover, by comparing the spectrum from a single C_{60} molecule and its molecular crystal, we find hints of the influence of solid-state effects on its electronic structure.

DOI: 10.1103/PhysRevLett.113.185502 PACS numbers: 81.05.ub, 68.37.Ma, 71.20.Tx, 79.20.Uv

The elucidation of molecular structure is generally performed by macroscopic methods, such as x-ray diffraction [1,2] or nuclear magnetic resonance [3], in which numerous identical molecules are required. In the current flurry of activity towards the realization of molecular devices [4–6], it becomes increasingly important to establish methods to identify individual molecules. Scanning tunneling microscopy and spatially resolved scanning tunneling spectroscopy have been used to characterize individual molecules. These techniques give access to electronic levels close to the Fermi level [7–9].

In order to identify individual molecules with different symmetry and to perceive their electronic structure modification under environment influence, core-level spectroscopy assessing the local environment of specific atomic species must be performed on a single-molecular basis. Electron energy-loss spectroscopy based on scanning transmission electron microscopy has so far been successfully used for the chemical analysis of individual metallofullerenes [10] (one or a few metal atoms encapsulated in a carbon cage), which however, requires only elemental information. More detailed spectral information, available in the energy-loss near edge fine structure (ELNES) technique, is a prerequisite to discriminate carbon cage structures with different symmetries.

Spectroscopy of isolated fullerenes without any support would be ideal to probe their pristine electronic structures. However, this is hardly feasible in an electron microscope, as the sample has to be stationary at the focal point of the microscope during imaging and spectroscopy. Alternatively, we have stored fullerenes in the thinnest possible materials: a single-wall carbon nanotube (SWNT) or in-between a boron nitride (BN) bilayer (Fig. 1). The former sample, namely, peapods, was prepared by codoping SWNT material with purified C_{60} and C_{70} in the vapor phase. The latter sandwich specimen was achieved by transferring a second atomic BN layer on top of a BN layer containing C_{60} molecules, deposited as droplets. After our experiments, we found out that the first option is better adapted for single molecular spectroscopy, as it minimizes molecular movement and deformation. The interactions of fullerene-fullerene and fullerene-nanotube are almost negligible due to the decreased contact surface area in peapods. On the other hand, the fullerene molecules on or between the BN bilayer are continuously moving under the electron beam until they start to aggregate.

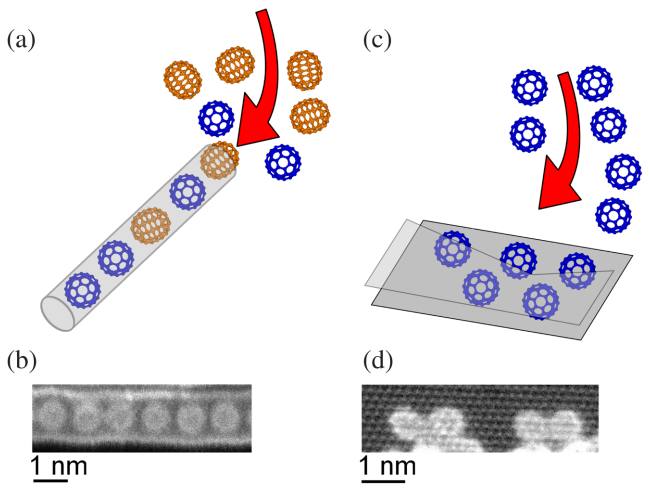

FIG. 1 (color online). [(a) and (b)] Model and annular dark field (ADF) images of C_{60} (blue, dark grey in print) and C_{70} (orange, light grey in print) molecules stored inside a SWNT. [(c) and (d)] Model and ADF images of C_{60} (blue) molecules stored between two layers of BN. The ADF image was taken at 30 kV for (b) and 60 kV for (d).

High spatial resolution EELS experiments using 30 and 60 keV electrons were performed on a JEOL 2100 F microscope equipped with JEOL Delta aberration correctors and a cold field emission gun (full width at half maximum of 0.35 eV) [11,12]. A Gatan Quantum spectrometer modified for low-energy operation was used. The convergence and EELS collection semiangles were 40 (48 mrad) and 63 (59 mrad) at 30 (60 keV), respectively. Typical electron beam currents during experiments were between 10 and 20 pA at 30 and 60 keV, respectively. The EELS spectrometer was set to 50 meV/channel dispersion. The spectra were calibrated by comparing our results to x-ray absorption spectroscopy (XAS) results from the literature [13] (Supplemental Material Fig. S1 [14]). Using this calibration the SWNT π^* peak energy was placed at 285.2 eV. Standard spectra for SWNT have been used to subtract the SWNT contribution from fullerenes spectra. These SWNT standards have been measured with a much higher exposure time than the molecular spectra (more than 60 s when compared to a few seconds per molecule). This ensured that the signal to noise ratio of the desired spectra was not limited by the subtraction procedure.

The identification of individual molecules must be performed with intact or minimally damaged structures. Since the use of high-energy incident electrons is known to induce molecular damage, decreasing the acceleration voltage is essential. Even using electrons with energy as low as 60 keV, the fullerenes are still punctured as the required dose for the individual molecular spectroscopy is quite high [11,15]. Though edge states of carbon atoms at graphene have been successfully captured using carbon K edge spectroscopy [12], such ELNES measurements require a signal to noise ratio 10 times higher than that for simple chemical analysis. Identifying specific carbon allotropes, possibly individual molecules with different symmetries, involves much higher energy resolution in the ELNES spectra and, therefore, much higher doses. To ensure the molecules survive the necessary dose for identification, we have employed here propitious 30 keV electrons for all the experiments unless otherwise stated.

To identify individual fullerene molecules, we have acquired 60 EELS spectra while scanning an electron beam of about 0.15 nm wide with a step increment of 0.07 nm along the tube axis, as indicated by an arrow in Fig. 2(a) (inset). This line spectrum contains the carbon K edge information of five fullerene molecules (as numbered). To retrieve the ELNES spectrum from each fullerene stored in SWNTs, we have subtracted the contribution of the SWNT from the total signal, assuming the carbon K edge spectrum can be considered as a simple sum of those of the fullerene and the SWNT (Supplemental Material Fig. S2 [14]). The same method has been used to retrieve the spectrum of C_{60} in peapods using x-ray absorption spectroscopy [16,17]. This hypothesis is reasonable, as the nanotube and the fullerenes interact weakly.

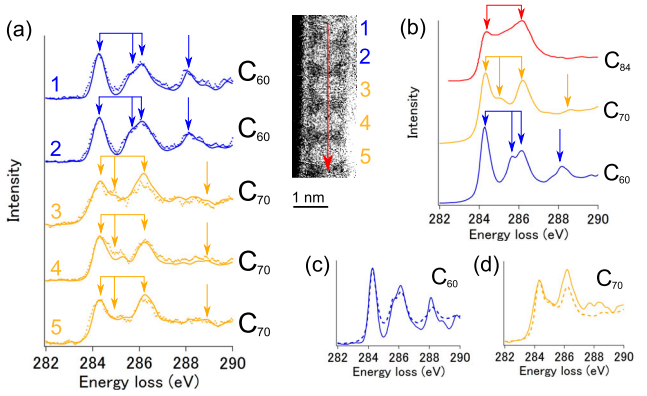

FIG. 2 (color online). (a) ELNES carbon K edge spectra extracted from five aligned molecules shown in the inset on the right. Note that the contribution of carbon nanotube to the carbon K edge spectra has been extracted by recording separately the carbon K edge of an empty nanotube. The solid lines are spectra after Richardson-Lucy deconvolution [18], and the dots are the raw data after background subtraction. Blue and orange arrows point to common features of C_{60} and C_{70}, respectively (see text). From these spectra peak configurations, the discrimination of C_{60} and C_{70} molecules is, indeed, possible. The same common features can be seen in (b), where reference spectra from crystalline C_{60}, C_{70}, and C_{84} are shown. The C_{84} spectra were extracted from Kuzuo *et al.* [19] and obtained at 60 kV, while the others were obtained at 30 kV, as in the other experiments described here. Reference spectra for C_{60} and C_{70} crystals have been deconvoluted using the maximum entropy method [20]. [(c) and (d)] Comparisons of the bulk crystalline spectrum (dashed lines) with a single molecule spectrum (solid lines) for C_{60} (blue) and C_{70} (orange), respectively.

In Fig. 2, the spectra of these five molecules after subtraction of the SWNT signal are compared (see blue and orange arrows) with the bulk reference spectra of C_{60} and C_{70} (raw spectra are shown in the Supplemental Material Fig. S2 [14]). To observe the energy-loss fine structures of C_{60} and C_{70} molecules, long exposure times were used (total time between 3 and 7 s per molecule) to obtain a SN ratio that is high enough to assign individual molecular structures. After comparison of these spectra with the bulk spectra of C_{60} and C_{70} crystals, we have concluded that the first two molecules in the inset of Fig. 2(a) are C_{60}, while the other three are C_{70}. This distinction is straightforward by looking at the near edge fine structure of the carbon K edge. Features from C_{60} and C_{70} molecules are pointed out by the arrows in Fig. 2(a). Two peaks are common to C_{60} and C_{70} molecules at 284.3 and 286.1 eV. In C_{60} additional peaks are observed at 285.6 and 288.2 eV (broader). The peak at 285.6 eV is measured as a shoulder of the 286.1 eV peak and can be clearly distinguished after Richason-Lucy deconvolution [18]. The C_{70} spectrum shows additional peaks at 284.8 and 288.5 eV (broad and weak peak). The 284.8 eV peak appears at slightly different energies for each C_{70} molecule. This might be due to the molecular orientation with respect

to the electron beam or the intramolecular positions we probed. Note that C_{60} molecules (I_h) have 60 equivalent atoms with only two bond types, while C_{70} molecules (D_{5h}) have five distinct atomic sites with eight bond types [21]. Therefore, the spectrum of C_{70} can be dependent on the molecular orientation and/or on which atoms are exactly probed in a spectrum. Calculations, in fact, suggest that for distinct atoms in the C_{70} molecule this peak appears at different energy and intensity (Supplemental Material Fig. S3 [14]) [22,23]. Sharp peaks in the π^* region tend to appear for lower-mass fullerenes due to their higher symmetry. These sharp features become broadened in higher-mass fullerenes with lower symmetry, such as C_{84} [Fig. 2(b) top] [19,21,24]. Similar identification of C_{60} molecules in a BN bilayer has also been attempted (Supplemental Material Fig. S4 [14]).

Spectra from individual C_{60} and C_{70} molecules are compared to references measured in bulk crystalline C_{60} and C_{70} in Figs. 2(c) and 2(d). The resemblance is unquestionable because the peak positions exactly match each other. This implies that the interaction between the fullerenes and the SWNT is quite small and that the encapsulated fullerenes suffer no massive distortion, retaining their original symmetry. However, in the case of C_{60}, the single molecule spectrum appears sharper; when the spectra are normalized by height of the peak at 284.3 eV, the dips at 285.0 and 287.2 eV are, indeed, deeper in the single molecule spectrum in comparison to those of the crystalline spectrum. Note that the bulk and individual spectra are taken exactly at the same settings of the microscope and spectrometer, such as acceleration voltage and energy dispersion (but not the same dose). The same tendency, sharper spectrum for individual molecules, is also confirmed when comparing our data to experiments with bulk C_{60} from the literature [19,21,24].

Even though the specimen was synthesized by codoping SWNTs with purified C_{60} and C_{70} fullerenes, we have successfully identified an impurity molecule stored in a SWNT. Over 100 molecules have been investigated within 17 SWNTs, but this is the unique confirmed case that we have found an unexpected contaminant. A set of the carbon K edge spectrum of four molecules aligned in another SWNT is shown in Fig. 3. Three of them can readily be identified as two C_{60} and one C_{70} molecule. The fourth one does not match the C_{60} or the C_{70} bulk spectra but shows a considerably broader peak suggesting a lower-symmetry fullerene molecule. In comparison with experimental data from bulk fullerenes (extracted from Ref. [19]), we found out that this C K edge resembles that of C_{84}. However, as broader peaks should be common for all higher fullerenes, we cannot definitely assign this molecule to C_{84}. Also, 24 isomers (2 major) for C_{84} exist, which cannot be discriminated from this spectrum. Still, it is clear that the assigned molecule is not C_{60} or C_{70} and that we have successfully detected an impurity molecule, what is not possible by any other spectroscopic method providing averaged spectra.

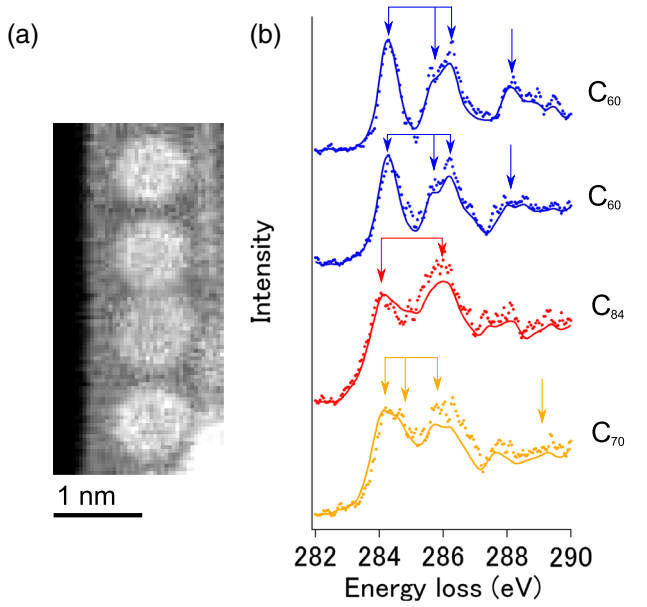

FIG. 3 (color online). (a) Representative ADF image of fullerenes in a SWNT. (b) Spectra of four molecules compared to experimental spectra from bulk. Two of the molecules are identified as C_{60} and one as C_{70}. The fourth molecule (red) spectrum shows broader peaks indicating a lower symmetry and closely matches that of C_{84} [shown in Fig. 2(b)], though not definitely assigned.

The ELNES spectra of molecules will change with the degree of irradiation damage under the electron beam. This is inevitable for techniques using high-energy incident particles, such as electrons or x-ray photons. For example, C K edge ELNES analyses of large quantities of molecules have shown that damage can be detected for doses as small as 2000 $e\,\mathrm{nm}^{-2}$ at 60 keV [25]. X-ray absorption near edge spectroscopy also allows element-specific information; however, the spatial resolution of x-ray spectroscopy is currently of the order of 50 nm [26]. For this reason, it is highly difficult to perform spectroscopy on targeted small molecules separated by 1 nm using X-ray absorption near edge spectroscopy.

In order to quantify the spectral evolution and the damage rate of fullerene crystals under electron beam irradiation, we performed chronospectroscopy of bulk crystals of C_{60} and C_{70} with the constant electron dose. The ELNES spectra were continuously monitored every 2 to 5 min when limited regions of each crystal, approximately 100 nm^2, were exposed to the electron beam of different energies (see the Supplemental Material Fig. S5 [14]). Some of the peaks are found to be very sensitive to the electron dose. Sharp features decrease as a function of dose. In order to quantify the spectrum sharpness as a function of those, we define here a spectrum contrast R [Fig. 4(a)]. This quantity as a function of dose for the bulk

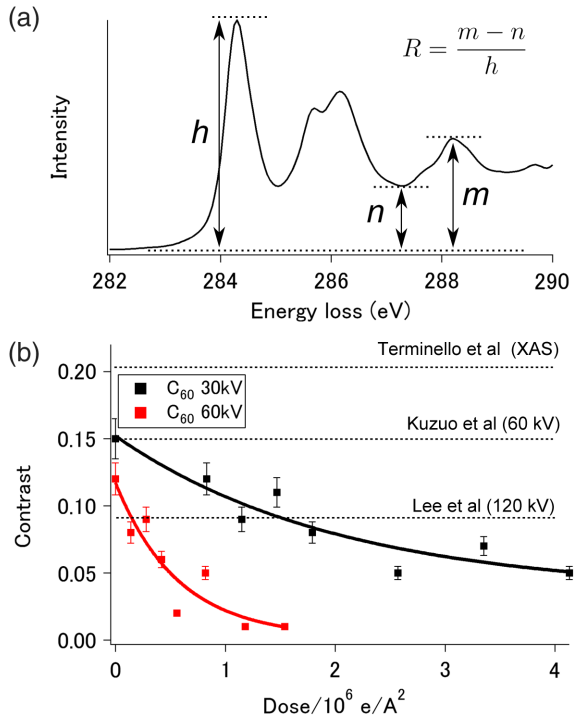

FIG. 4 (color online). Quantification of irradiation damage under the electron beam with increasing dose. (a) Definition of a spectrum contrast R as the ratio between $m - n$ (288.2 eV peak height) to h (284.3 eV peak height). (b) Spectrum contrast R as a function of dose for experiments using 30 keV (black) and 60 keV (red) electrons derived from the chronospectroscopy of C_{60} bulk crystals (see Supplemental Material Fig. S5 [14]). The dashed lines mark the contrast measured from data in the literature [19,21,24].

C_{60} crystals at 30 and 60 keV is shown in Fig. 4(b). The damage rate is very fast at 60 keV while R decreases more moderately at 30 keV. Therefore, fullerenes experiments should be performed at 30 keV or lower to preserve the molecular structures [27].

Our reference spectra were acquired with the smallest possible dose in pristine thin crystal regions and using 30 keV electrons. In these conditions, the molecules should have suffered very little damage. In Figs. 2(c) and 2(d), the single molecule shows much higher spectrum contrast ($R \sim 0.40$) than the pristine bulk. This is surprising because the relative electron dose per molecule can be quite higher for single-molecule experiments ($\sim 1 \times 10^7\ e/\text{Å}^2$). A simple explanation can be due to the solid-state effect that broadens peaks in the bulk spectra. This can, indeed, be expected for C_{60} molecular crystals, as energy band calculations [28,29] show that discrete molecular levels become broader energy bands in crystals.

We note that the definition of spectrum contrast depends on the resolution of the spectrometry. Hence, comparisons between different experiments cannot be fully appropriate because lower spectrum contrast might simply mean worse spectral resolution. Despite this, our ELNES spectrum of bulk C_{60} crystal is almost identical to that measured by XAS [13] (Supplemental Material Fig. S1 [14]). This, indeed, means that spectrum resolution of EELS based on scanning transmission electron microscopy is now compatible to that of XAS using a synchrotron. In Fig. 4(b) we have also marked the spectrum contrast for C_{60} from the literature. The higher contrast of the XAS data may be explained by higher spectral resolution. The same contrast is observed in our experimental data after Richardson-Lucy deconvolution. The inferior spectrum contrast observed in the literature (Lee *et al.* [21]) could have occurred because of quicker electron beam damage at 120 keV, as damage destroys the original symmetry. The reaction of fullerenes under the influence of the electron beam has been reported before [30], and we can expect dimerization and fusion of adjacent fullerenes for the first stage of electron beam damage, which massively degrades the molecular symmetry.

We have found that the C_{60} molecules that are anchored and sandwiched by BN bilayers tend to show large modifications of their spectra compared to those of the intact fullerenes. In principle, the C_{60} molecules are not fixed on BN layer but continuously mobile during observation, and one cannot perform the core-level spectroscopy on these. When the C_{60} molecules start to aggregate, the spectra are no longer sharp, possibly due to the interactions with neighbors and consequently the degraded symmetry (Supplemental Material Figs. S4 and S5 [14]). The process of adding the second BN layer may also induce deformation by compressing the molecules due to the force between the two BN layers. Such modified electronic structures due to symmetry breakage can be also expected in single-molecular devices with electrodes but will never be perceived by a spectroscopic method that provides only averaged spectra.

Our results show that low-energy ELNES is a viable tool to identify single molecules with nanometer spatial resolution. In fact, the association of high spectral and spatial resolutions makes ELNES using low accelerating voltages a unique tool to probe heterogeneous molecular samples. Single molecule spectroscopy has been also performed at nanometer spatial resolution by plasmon-enhanced Raman spectroscopy [31] and scanning tunneling spectroscopy [32,33]. However, these methods probe valence electrons in the infrared to ultraviolet energy range, possessing no element-specific information. Comparison of our spectral resolution to spectra from Ref. [24] indicates that differentiating C_{60}, C_{70}, C_{76}, and C_{84} inside a SWNT could be feasible. Moreover, two-dimensional mapping of carbon atoms with different chemical bonds within a single molecule may be possible. One could envisage discerning C=C, C-O, or C-H bonds based on ELNES in molecules. Such experiments require sophisticated electron optics, and they might become feasible even in a SEM in the near future. Access to higher spectral resolution, such as electron monochromators, at lower electron beam energies

will lead to the mapping of even finer structures and vibrational modes in individual molecules. The vibrational electron spectroscopy of fullerene crystals has been demonstrated in the past [34].

Yoshiko Niimi, Kayoko Sato, and Haruka Kobayashi are gratefully acknowledged for their assistance of specimen preparations and TEM observations. This work is partially supported by the JST Research Acceleration Programme. Financial support by JSPS KAKENHI Grants No. 23681026 and No. 26390004 is acknowledged by M. K. Financial support by Grant-in-Aid for Scientific Research on Innovative Areas (MEXT KAKENHI Grant No. 25107003) is acknowledged by Z. L.

*suenaga-kazu@aist.go.jp

[1] B. D. Cullity, *Elements of X-Ray Diffraction* (Addison-Wesley Publishing Company, Reading, MA, 1978).
[2] S. Boutet *et al.*, Science **337**, 362 (2012).
[3] R. K. Harris, R. E. Wasylishen, and M. J. Duer, *NMR Crystallography* (Wiley, New York, 2009).
[4] M. A. Reed, C. Zhou, C. J. Muller, T. P. Burgin, and J. M. Tour, Science **278**, 252 (1997).
[5] M. Tsutsui, S. Rahong, Y. Iizumi, T. Okazaki, M. Tanighuchi, and T. Kawai, Sci. Rep. **1**, 46 (2011).
[6] A. Y. Kasumov *et al.*, Phys. Rev. B **72**, 033414 (2005).
[7] B. C. Stipe, M. A. Rezaei, and W. Ho, Science **280**, 1732 (1998).
[8] M. Grobis, K. H. Khoo, R. Yamachika, X. Lu, K. Nagaoka, S. G. Louie, M. F. Crommie, H. Kato, and H. Shinohara, Phys. Rev. Lett. **94**, 136802 (2005).
[9] L. Liu, S. Liu, X. Chen, C. Li, J. Ling, X. Liu, Y. Cai, and L. Wang, Sci. Rep. **3**, 3062 (2013).
[10] K. Suenaga *et al.*, Science **290**, 2280 (2000).
[11] K. Suenaga *et al.*, Nat. Chem. **1**, 415 (2009).
[12] K. Suenaga and M. Koshino, Nature (London) **468**, 1088 (2010).
[13] L. J. Terminello, D. K. Shuh, F. J. Himpsel, D. A. Lapiano-Smith, J. Stohr, D. S. Bethune, and G. Meijer, Chem. Phys. Lett. **182**, 491 (1991).
[14] See Supplemental Material at http://link.aps.org/supplemental/10.1103/PhysRevLett.113.185502 for details.
[15] O. L. Krivanek, N. Dellby, M. F. Murfitt, M. F. Chisholm, T. J. Pennycook, K. Suenaga, and V. Nicolosi, Ultramicroscopy **110**, 935 (2010).
[16] X. Liu, T. Pichler, M. Knupfer, M. S. Golden, J. Fink, H. Kataura, Y. Achiba, K. Hirahara, and S. Iijima, Phys. Rev. B **65**, 045419 (2002).
[17] C. Kramberger, P. Ayala, H. Shiozawa, F. Simon, A. Friedrich, X. Liu, M. Rümmeli, Y. Miyata, H. Kataura, P. Hoffmann, and T. Pichler, Phys. Rev. B **83**, 195438 (2011).
[18] A. Gloter, A. Douiri, M. Tence, and C. Colliex, Ultramicroscopy **96**, 385 (2003).
[19] R. Kuzuo, M. Terauchi, M. Tanaka, Y. Saito, and H. Shinohara, Phys. Rev. B **49**, 5054 (1994).
[20] R. Egerton, *Electron Energy-Loss Spectroscopy in the Electron Microscope* (Springer, New York, 2011).
[21] S. M. Lee, R. J. Nicholls, D. Nguyen-Manh, D. G. Pettifor, G. A. D. Briggs, S. Lazar, D. A. Pankhurst, and D. J. H. Cockayne, Chem. Phys. Lett. **404**, 206 (2005).
[22] C. Herbert, Micron **38**, 12 (2007).
[23] J. P. Perdew, K. Burke, and M. Ernzerhof, Phys. Rev. Lett. **77**, 3865 (1996).
[24] M. Terauchi and M. Tanaka, J. Surf. Anal. **3**, 240 (1997).
[25] M. M. van Schooneveld, A. Gloter, O. Stephan, L. F. Zagonel, R. Koole, A. Meijerink, W. J. M. Mulder, and F. M. F. de Groot, Nat. Nanotechnol. **5**, 538 (2010).
[26] A. P. Hitchcock *et al.*, Ultramicroscopy **88**, 33 (2001).
[27] K. Suenaga, Y. Iizumi, and T. Okazaki, Eur. Phys. J. Appl. Phys. **54**, 33508 (2011).
[28] M. S. Golden, M. Knupfer, J. Fink, J. F. Armbruster, T. R. Cummins, H. A. Romberg, M. Roth, M. Sing, M. Schmidt, and E. Sohmen, J. Phys. Condens. Matter **7**, 8219 (1995).
[29] S. Saito and A. Oshiyama, Phys. Rev. Lett. **66**, 2637 (1991).
[30] M. Koshino, Y. Niimi, E. Nakamura, H. Kataura, T. Okazaki, K. Suenaga, and S. Iijima, Nat. Chem. **2**, 117 (2010).
[31] R. Zhang *et al.*, Nature (London) **498**, 82 (2013).
[32] D. Porath and O. Mill, J. Appl. Phys. **81**, 2241 (1997).
[33] E. Shapir, H. Cohen, A. Calzolari, C. Cavazzoni, D. A. Ryndyk, G. Cuniberti, A. Kotlyar, R. Di Felice, and D. Porath, Nat. Mater. **7**, 68 (2008).
[34] Y. Fujikawa, K. Saiki, and A. Koma, Surf. Sci. **357–358**, 176 (1996).